Applied Occupational and Environmental Hygiene

ISSN: 1047-322X (Print) 1521-0898 (Online) Journal homepage: http://www.tandfonline.com/loi/uaoh20

A Model to Estimate Worker Exposure to Spray Paint Mists

Gary N. Carlton & Michael R. Flynn

To cite this article: Gary N. Carlton & Michael R. Flynn (1997) A Model to Estimate Worker Exposure to Spray Paint Mists, Applied Occupational and Environmental Hygiene, 12:5, 375-382, DOI: 10.1080/1047322X.1997.10389521

To link to this article: https://doi.org/10.1080/1047322X.1997.10389521

Published online: 25 Feb 2011.

A Model to Estimate Worker Exposure to Spray Paint Mists

Gary N. Carlton and Michael R. Flynn

Department of Environmental Sciences and Engineering, University of North Carolina at Chapel Hill, Chapel Hill, North Carolina 27599

Exposure models traditionally have emphasized the statistical association between process parameters and measured exposures. These empirical–statistical models can identify factors important in controlling exposure, but are difficult to generalize for various reasons. Different modeling techniques may have wider applicability. Known as empirical–conceptual models, they are based on a conceptual analysis that identifies contaminant generation and transport processes leading to the exposure. Dimensional analysis is used to group important process parameters into independent, nondimensional ratios. The relationship among these ratios is then determined from experiment. This research develops an empirical–conceptual model of exposure to mists generated during a spray painting task. Dimensional analysis is used to identify four important dimensionless quantities. Laboratory wind tunnel experiments with a mannequin, flat plate, and spray nozzle provided data to determine the mathematical relationship between these quantities. The model successfully explained the variability in the average breathing zone concentration of the mannequin within measurement uncertainty. Mannequin orientation to the freestream had a significant effect on breathing zone concentrations. A dimensionless quantity consisting of spray nozzle pressure, mannequin height, liquid viscosity, and average freestream velocity determined in which orientation the breathing zone concentration was higher. Differences between the experimental setup and actual spraying tasks may limit application of the model. However, the research indicates good potential for empirical–conceptual models based on dimensional analysis to predict breathing zone concentrations. This should lead to more effective control interventions and reduced exposures. CARLTON, G.N.; FLYNN, M.R.: A MODEL TO ESTIMATE WORKER EXPOSURE TO SPRAY PAINT MISTS APPL. OCCUP. ENVIRON. HYG. 12(5):375–382; 1997.

A primary goal of industrial hygiene is to control worker exposure to hazardous materials and prevent occupational disease. If inhalation is the route of exposure, then hygienists typically base judgments for appropriate control measures on breathing zone sampling. In some cases, references are available that outline effective controls for specific hazards, for example, the American Conference of Governmental Industrial Hygienists (ACGIH Industrial Ventilation: A Manual of Recommended Practice).[1] Another less frequently used method for evaluating control options is exposure modeling.

There are two types of exposure models: theoretical and empirical. Theoretical models use computational fluid dynamics to solve the basic governing equations determining the distribution of contaminants in air. However, these equations are intricate and analytical solutions are impossible. Current capabilities limit numerical results to relatively simple situations which do not reflect the complexity of most industrial operations.

Empirical models address this complexity by relating the exposure to various process parameters. Kromhout *et al.*[2] sampled the rubber manufacturing industry in The Netherlands and correlated exposures to tasks performed, ventilation characteristics, and production variables. Woskie *et al.*[3] looked at exposures to metalworking fluids in automotive component manufacturing and developed a model based on several factors, including the fluid type, the presence or absence of local exhaust, and the atmospheric conditions. Kromhout called this the empirical–statistical approach since the model relates exposure to the parameters by multiple linear regression. It is difficult to apply these models to new situations, however, since additional factors, not considered in developing the model, may be important. Also, the assumption of linearity between exposure and causal factors may leave much of the variability unexplained since there is no guarantee that the dependence is linear. In addition, factors that do not vary much during sampling will not show up in the model, even though they may be important in controlling the exposure.

A different type of empirical model relates the exposure to the process parameters, not by their statistical association, but through a conceptual model. This empirical–conceptual approach is appropriate if a limited number of identifiable factors determine the exposure. A conceptual model of the industrial operation is developed, outlining contaminant generation and transport processes leading to the exposure. Each process is examined and factors that characterize it are identified. Once these factors are known, an empirical model results from dimensional analysis, a process of grouping the factors into nondimensional ratios and performing experiments to determine the relationship between these ratios. Besides improving physical insight into the problem, this method has the potential to generalize the model to new situations.[4] The model does not require an assumption of linearity. Furthermore, as long as a sound conceptual understanding of the problem exists, the model should include all factors important to controlling the exposure.

Spray painting tasks are well suited to test whether an empirical–conceptual model can predict worker exposures. Spraying paint gives workers good control over the quality of finish, but results in exposure to paint mists. Even though

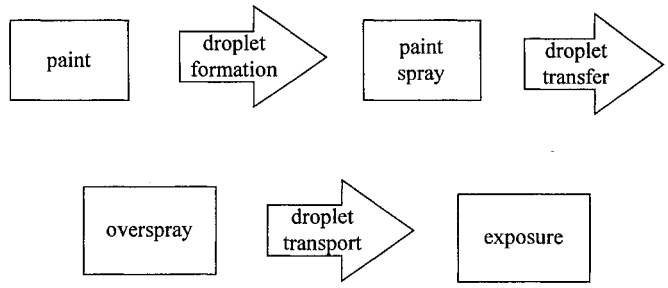

FIGURE 1. Conceptual model of a spray painting task showing the sequential processes resulting in exposure.

generation of this mist and its interaction with the flow field in a paint spray booth are complex, a limited number of factors determine the exposure. Spray painting tasks lend themselves to modeling since these factors are identifiable.

This research develops an empirical–conceptual model to predict breathing zone concentrations of paint mist during spray painting tasks. If validated in the field, this model will allow the industrial hygienist to identify work practice changes and improve the efficiency of engineering controls. Although spray painting is the process of interest, the modeling concepts developed here should have applicability to other industrial operations as well.

Conceptual Model

The spray application process of most concern from an exposure viewpoint is compressed air atomization. Also known as pneumatic or twin-fluid atomization, it is the most widely used spray application process in industry.[5] It is popular because it can atomize viscous liquids like paint and adjust the atomization quality by varying air and liquid flow rates to the atomizer. Compressed air atomization is classified as either conventional or high volume, low pressure (HVLP) spraying. Conventional spraying operates at air pressures greater than 20 psig, while HVLP spraying involves lower pressures, usually 10 psig or less.

Compressed air atomization produces a paint mist which can enter a worker's breathing zone and lead to an exposure. This exposure results from three sequential processes common to all spraying tasks, shown conceptually in Figure 1.

The droplet formation process produces the droplets that coat the workpiece. A spray gun causes compressed air to interact with the paint and form droplets. Paint atomizers are universally external mixing, meaning the paint and air interact outside of the atomizer. They are also generally parallel flow, characterized by the atomizing air and liquid flowing in the same direction when they contact. The spray gun discharges the liquid through a fluid nozzle, and a hollow column of air emitted from the air nozzle surrounds this liquid stream. Shear forces develop along the surface of contact between the two fluids, causing the liquid to disintegrate into droplets.[6] This interaction is complex, and empirical observations are the primary basis for knowledge of the resulting particle size distributions.[7] The most important factors affecting these distributions are: air pressure at the nozzle (p_n); liquid paint viscosity (μ_l); and ratio of air to liquid mass flow rates (m_a/m_l).[7–9]

The droplet transfer process creates the paint mist or overspray. The air jet leaving the spray gun imparts a forward velocity to the droplets. This jet produces an air flow pattern around the workpiece. Larger droplets deviate from the air flow streamlines and deposit on the object. Smaller droplets with insufficient momentum to deposit follow the streamlines and become entrained in the air flow around the object to form the overspray (m_o). The transfer efficiency of the spray, or the fraction of droplets that impact on the workpiece, depends primarily upon droplet momentum and the distance from the spray gun to the object.[9,10] Droplets receive momentum from the velocity of the air jet, which for compressed air atomizers results from the nozzle air pressure (p_n). Spray gun-to-object distances do not vary much among compressed air painting tasks; guidelines recommend keeping the gun within 6 to 8 inches of the object.[5]

In the final process, droplet transport, the overspray may enter the worker's breathing zone. This is typically the stage where intervention takes place to control the exposure. This is usually local exhaust ventilation if painting occurs in a spray booth. ACGIH recommends ventilation rates as average freestream velocities (U).[1] Small booths encompass the workpiece and capture the overspray like an enclosing hood. Larger booths allow the worker to stand in the freestream while painting. The freestream propels the overspray toward one end of the booth, where an air-cleaning device, usually a dry filter bed or water curtain, removes the droplets. The worker generally orients the workpiece so the freestream is either to the worker's side (90° orientation) or to the worker's back (180° orientation; see Figure 2). The uniform freestream can cause a boundary layer to form around the worker and a reverse flow region to develop downstream of the worker.[11] Contaminants generated in this wake can move into the breathing zone when the worker is in the 180° orientation.[12] Investigators document a difference in breathing zone concentration (C) when a mannequin of height H and breadth D is positioned in these two orientations and holds a passive contaminant source.[13,14] This research emphasizes these larger spray booths where this orientation effect may also be important.

Droplet evaporation proceeds concurrently with droplet transfer and transport. Overspray droplets decrease in size as the solvent fraction volatilizes. This change in size distribution affects the movement of the overspray and results in worker exposure to solvent vapors, though vapor concentrations are generally low during spraying tasks if ventilation is available.[15–19] The overspray, consisting of paint solids and unevaporated solvent, contributes most of the worker's total mass exposure. This research develops an empirical model based on dimensional analysis for this overspray contribution to the exposure.

Empirical Model Development

The overspray leads directly to the worker's exposure. Controlling this overspray will result in lower breathing zone concentrations and reduced exposures, all other factors being equal. A successful model based on the overspray generation rate should lead to better control measures and allow application to a wide variety of spraying tasks.

The primary hypothesis is that the worker's average breathing zone concentration during a spraying task is a mathematical function of the factors defining the conceptual model shown in

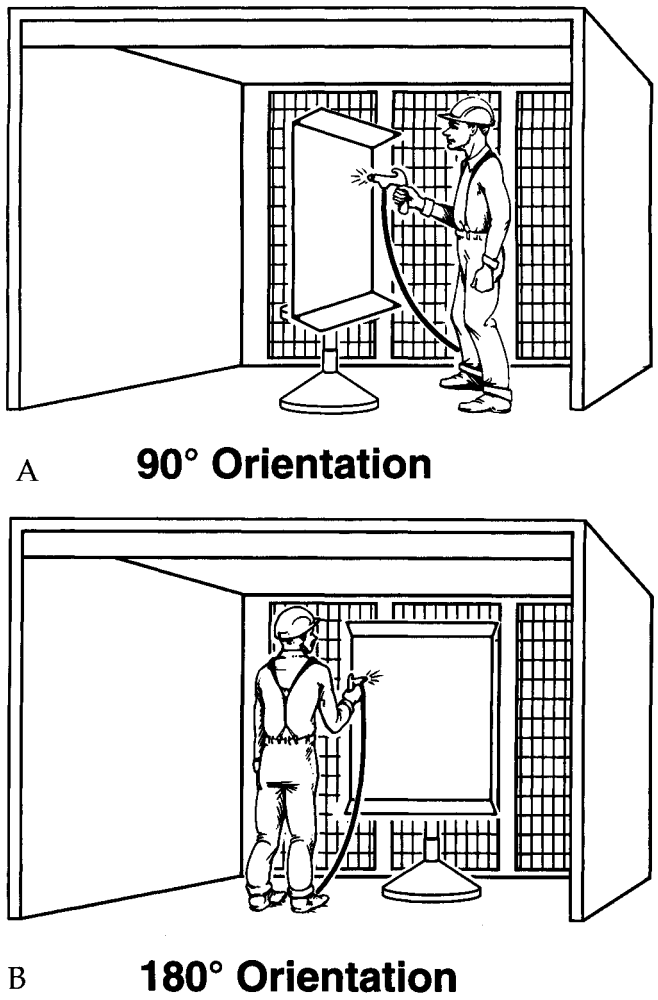

FIGURE 2. Worker orientation to the freestream. In the 90° orientation the freestream flows to the worker's side; in the 180° orientation, to the worker's back.

Figure 1. These factors are: overspray mass generation rate; spray nozzle pressure; paint viscosity; ratio of air-to-liquid mass flow rates; freestream velocity; dimensions of the worker; and worker orientation to the freestream. The following equation represents the functional dependence between these nine variables:

$$C = \phi(m_o, p_n, \mu_l, m_a/m_l, U, H, D, \text{orientation}) \quad (1)$$

Since Newton's second law is not specifically included in the problem formulation, the FMLT measuring system reveals the nondimensional form of this relationship. This system designates four primary quantities (force, mass, length, and time). The Buckingham pi theorem states that the number of independent dimensionless groups equals the difference between the number of initial factors and the number of primary quantities.[4] Therefore, five nondimensional variables describe the functional relationship between the nine factors pertinent to a spray painting task. A dimensional analysis after selecting m_o, μ_l, U, and H as the four repeating variables which do not by themselves form a dimensionless group provides the following nondimensional representation of the problem:

$$CUH^2/m_o = \Phi(m_a/m_l, p_nH/\mu_lU, H/D, \text{orientation}) \quad (2)$$

Assuming that the ratio of body height to breadth is fairly constant among workers[20] reduces the number of dimensionless groups by one and results in the final model:

$$CUHD/m_o = \Phi(m_a/m_l, p_nH/\mu_lU, \text{orientation}) \quad (3)$$

The dimensional analysis indicates that under similar flow conditions, the concentration group $CUHD/m_o$ is a function of worker orientation to the freestream and two other nondimensional groups. The previously identified group, m_a/m_l, influences droplet size distributions from pneumatic nozzles.[7,8] The second group, p_nH/μ_lU, is new. This dimensionless quantity incorporates four important elements of the task: the spray gun (p_n), the paint (μ_l), the spray booth (U), and the worker (H).

Methods

Laboratory Setup

A laboratory model of a spray painting task was used to determine the relationship between the nondimensional groups. Spraying took place in a wind tunnel which simulated a paint spray booth. The tunnel has a cross-sectional area of 25 ft^2 and is 8 ft deep. Uniform velocity profiles due to a flared entrance flange and a pegboard rear wall were confirmed with hot wire anemometry. Average freestream velocities (U) from 75 to 350 ft/min with a longitudinal component of freestream turbulence intensities of 6 to 11 percent are possible in the tunnel.

The laboratory model used a Spraying System 1/4J spray nozzle fitted with a 60100 fluid cap and 120 air cap. The nozzle consists of an annulus for air flow (area of 0.00346 $inches^2$) surrounding a circular orifice for the liquid flow (area 0.00283 $inches^2$). This pneumatic, external-mixing spray nozzle operates at nozzle pressures and air-to-liquid mass flow ratios similar to a compressed air spray gun and produces comparable droplet size distributions, characterized by Kim and Marshall.[8] The nozzle was operated in either the gravity feed or siphon configuration. Changing the gravity feed or siphon height of a liquid container varied the liquid mass flow rate (m_l) to the nozzle, measured by weighing the container before and after spraying. A compressed air source provided air for the nozzle. A pressure regulator adjusted the nozzle pressure (p_n) and air mass flow rate (m_a). Fixing the nozzle pressure and adjusting the liquid container height set the air-to-liquid mass flow ratio (m_a/m_l).

A mannequin 41 inches in height (H) and 8 inches in breadth (D) simulated the worker. A flat plate the same height as the mannequin represented the workpiece. A flat plate produces a uniform air jet rebound and forms a reproducible overspray generation rate. Flat plates would seem a reasonable model for many common objects such as jet engines, wing flaps, refrigerators, and vehicles, since the air rebound from the surface facing the worker is similar to a flat plate. The spray nozzle was at the position of the mannequin's right hand (upstream in the 90° orientation), 8 inches from the flat plate.

Corn oil was used to simulate the paint. It is nonvolatile and combines safety, low cost, and good simulation of paint properties. Since it is a natural product, a single manufacturer

provided corn oil to reduce variations in physical properties. The liquid viscosity (μ_l) varied from 39.8 to 55.2 centipoise due to liquid temperature changes, typical values for an enamel paint.

Overspray Generation Rate

Corn oil that impacted the flat plate during spraying drained into a trough located beneath it. The difference in trough weight before and after spraying determined the mass of corn oil transferred to the plate. The overspray generation rate (m_o) was the difference between the liquid mass flow rate (m_l) and the rate of corn oil transfer to the plate.

Breathing Zone Concentration

Samples were weighed in accordance with National Institute for Occupational Safety and Health (NIOSH) Method 0500 for total aerosol mass (37-mm polyvinyl chloride membrane filters with 5-μm pore size, sampled at 2.0 L/min)[21] to determine mannequin breathing zone concentration (C). The concentration obtained by this method may differ from the true aerosol concentration due to sampling error.[22] Among the important errors are the inlet sampling efficiency of the cassette affected by the aerosol size distribution, ambient air velocity, and sampler orientation;[23–27] transport loss from deposition on the cassette walls;[24,28,29] filter collection efficiency;[30] and evaporative loss from the filter during sampling.[31] The inhalable dust sampler developed at the Institute of Occupational Medicine addresses the transport loss problem by weighing the filter and cassette as a single unit, but the high tare weight of the cassette makes it unsuitable for monitoring short-term tasks where the collected mass is less than about 0.5 mg.[28] In addition, efficiency curves for this sampler are averaged over all orientations to the freestream to be compatible with the definition of inhalability.[24,27] Since orientation was a primary factor in the model, the NIOSH sampling method was preferred since sampling efficiencies in the 90° and 180° orientations are known,[26] allowing inferences on the effect of sampling error on the results. Since previous sampling conducted during industrial paint spraying operations showed that closed-face sampling potentially underestimates the overall worker exposure,[32] all sampling was in the open-face mode. The collection efficiency of 5-μm pore size filters for particles that contribute to the mass exposure (greater than 1 μm diameter) is essentially complete.[30] The use of nonvolatile corn oil reduced evaporative loss from the filter during sampling. A Cahn model 27 electrobalance with 0.001 mg sensitivity determined filter weights. Spraying lasted long enough to ensure adequate mass collection using the NIOSH recommended range of 0.1 to 2.0 mg as a guide, usually 5 to 10 minutes. The sampling cassette was placed at the mouth of the mannequin.

Experimental Design

The three independent dimensionless groups—m_a/m_l, p_nH/μ_lU, and orientation—were varied to determine their functional relationship with the dependent nondimensional concentration group, $CUHD/m_o$. The air-to-liquid mass flow ratios were 0.70, 0.90, and 1.30. There were two worker orientations, either 90° or 180° to the freestream. The nozzle pressure and wind tunnel velocity varied from 20 to 50 psig and 75 to 200 ft/min, respectively, providing p_nH/μ_lU values from 2.76×10^6 to 2.12×10^7. p_nH/μ_lU varied over ten experimental values for each value of m_a/m_l and orientation, giving a total of 60 experimental trials. Each trial had three replicates for a sum of 180 experimental runs. Conventional air guns operate in the range of 30 to 80 psig and with paint viscosities of 30 to 70 centipoise. For people 5 to 6 ft tall and actual spray booth air velocities in the range of 50 to 100 ft/min, this results in p_nH/μ_lU values from 5.9×10^6 to 1.3×10^8.

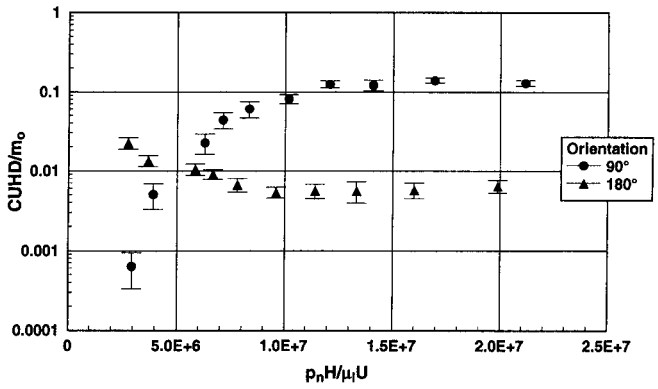

FIGURE 3. Functional relationship between the nondimensional groups identified by dimensional analysis as important to a spraying task.

Results

Figure 3 shows the functional relationship of p_nH/μ_lU to the concentration group $CUHD/m_o$ for the two worker orientations to the freestream. The points shown are averages of the nine runs (three replicates of three m_a/m_l values) for each p_nH/μ_lU value. The error bars represent one standard deviation. The orientation curves cross when p_nH/μ_lU equals 5.0×10^6. $CUHD/m_o$ is higher in the 90° orientation if p_nH/μ_lU exceeds 5.0×10^6, but if p_nH/μ_lU is less than 5.0×10^6, then $CUHD/m_o$ is higher in the 180° orientation.

A regression analysis found the following best-fit curves:

$$90° \text{ orientation: } CUHD/m_o = 1/\{7.44 + 1.08 \times 10^2 \exp[-5.64 \times 10^{-7}(p_nH/\mu_lU)]\}$$

$$r^2 = 0.98 \quad (4)$$

$$180° \text{ orientation: } CUHD/m_o = 3.23 \times 10^{-2} \exp[-1.94 \times 10^{-7}(p_nH/\mu_lU)], \; p_nH/\mu_lU < 10^7$$

$$r^2 = 0.95 \quad (5)$$

$$CUHD/m_o = 0.006, \; p_nH/\mu_lU > 10^7 \quad (6)$$

Based on the excellent fit of the data to the curves, m_a/m_l was not considered a significant factor in either orientation.

A measurement uncertainty analysis estimated the bias (fixed) and precision (random) experimental error in the nondimensional groups.[33] Bias is the systematic error constant for the duration of the experiment, which was minimized in this experiment by instrument calibration. The bias limit (B) is the

TABLE 1. Estimated Measurement Error and Uncertainty in Nondimensional Groups (Percent)

Nondimensional Group	Bias Error	Precision Error	Uncertainty (95%)
$CUHD/m_o$	4.49	6.07	12.94
p_nH/μ_lU	6.78	3.57	9.85
m_a/m_l	2.40	0.89	2.99

upper limit of this bias error. Precision is the closeness of agreement between repeated measurements of the same quantity. Precision is usually measured by the precision index of the measurements (S_X), the estimated standard deviation of the average of N measurements. Table 1 lists these estimates along with their calculated uncertainties, defined as:[33]

$$\text{uncertainty (95\%)} = [B^2 + (tS_X)^2]^{1/2} \quad (7)$$

where t is the 97.5th percentile of the two-tailed t-distribution with N degrees of freedom. For large samples t approaches 1.96 and is approximated as 2.0 for simplicity. The uncertainty in $CUHD/m_o$ is primarily due to inaccuracy in the NIOSH sampling method (±11%). An illustration and further discussion of the uncertainty estimates are presented in the Appendix.

Discussion

The results shown in Figure 3 provide an empirical exposure model. Worker orientation and the nondimensional group p_nH/μ_lU explain the variability in the average value of the concentration group $CUHD/m_o$ within the measurement uncertainty of the experimental setup. The fact that m_a/m_l was not significant is related to the fact that it is important in defining the droplet size distribution. This impacts transfer efficiency, and since the model uses the overspray generation rate, this has, to a large extent, already been incorporated into the model. Research is underway to evaluate the impact of size distribution on worker exposure and to clarify the transfer efficiency issue.

As mentioned earlier, the measured breathing zone concentration may be less than the actual concentration due to sampling error. As a result, the actual values of $CUHD/m_o$ may be higher than indicated in Figure 3, meaning that the orientation curves are shifted down from their true values. However, this inlet-aspiration sampling error is generally greater in the 90° orientation than the 180° orientation at the freestream velocities used in this experiment.[26] This means the measured values of $CUHD/m_o$ would be reduced more in the 90° orientation than in the 180° orientation. Therefore, the 90° orientation curve in Figure 3 is shifted down more than the 180° orientation curve. Even with this greater sampling error in the 90° orientation, the two orientation curves do not overlap within experimental error except at their crossover point. This leads to the conclusion that the orientation curves are different.

The most striking result apparent from Figure 3 is the importance of worker orientation to the freestream. George *et al.*[11] identified an orientation effect for a passive contaminant source (tracer gas) released near a mannequin in a wind tunnel. They found higher breathing zone concentrations in the 180° orientation for all wind tunnel velocities (49 to 265 ft/min). The situation for an aerosol injected with significant momentum into a flow field is more complex. For a given nozzle pressure, liquid viscosity, and average freestream velocity, the mannequin's breathing zone concentration is higher in the 90° orientation if p_nH/μ_lU exceeds 5.0×10^6, but higher in the 180° orientation when p_nH/μ_lU is less than this value. This runs counter to common industrial hygiene recommendations to place contaminant sources between the worker and exhaust to lower exposures. At least in the laboratory, this rule is invalid for low values of p_nH/μ_lU.

Observation of the spraying task provides an explanation for the crossover effect. At high nozzle pressures (corresponding to larger values of p_nH/μ_lU) and the mannequin in the 90° orientation, the air jet propelled some of the overspray droplets toward the wind tunnel entrance (see Figure 4). The freestream eventually captured these droplets, reversing them back into the wind tunnel and through the mannequin's breathing zone. In the 180° orientation the air jet appeared to overwhelm any reverse flow effect and prevented droplets from entering the worker's wake; the freestream captured the droplets before they could enter the breathing zone. The result was higher breathing zone concentrations in the 90° orientation when nozzle pressures were high. On the other hand, when nozzle pressures were low (corresponding to smaller values of p_nH/μ_lU), the freestream captured the droplets quickly and few entered the mannequin's breathing zone in the 90° orientation. However, in the 180° orientation separation downstream from the mannequin possibly became important. The droplets' low momentum allowed them to enter the worker's wake and caused increased breathing zone concentrations. The end result was higher breathing zone concentrations in the 180° orientation at lower nozzle pressures.

Although the influence of freestream velocity on breathing zone concentrations was not the primary purpose of this experiment, an interesting trend was observed in the 180° orientation. For a fixed nozzle pressure, the concentration increased as the velocity increased. This was apparent at all nozzle pressures but was most pronounced at the lowest nozzle pressure of 20 psig. This agrees with the findings of Kim and Flynn[34] that increases in freestream velocity may lead to higher breathing zone concentrations in the 180° orientation. This trend was not apparent in the 90° orientation; in all cases, increased ventilation reduced mannequin breathing zone concentrations. Although additional testing is necessary, these trends again indicate the importance of worker orientation.

Several limitations restrict applicability of the model to field spraying tasks. The laboratory setup was static and spraying was continuous. In actual spraying tasks, the worker and spray gun move and spraying is intermittent. The spray gun-to-target distance varies during the task and is not fixed as in this experiment, though it is poor practice to vary this distance much since it results in a poor-quality finish. A flat plate may not be representative of the workpiece. A nonvolatile liquid simulated paint; in the field, solvent evaporation may result in lower breathing zone concentrations than the model predicts. Most importantly, the available wind tunnel limited the laboratory setup to a reduced-scale mannequin and workpiece. Even though the spray nozzle air and liquid mass flow rates

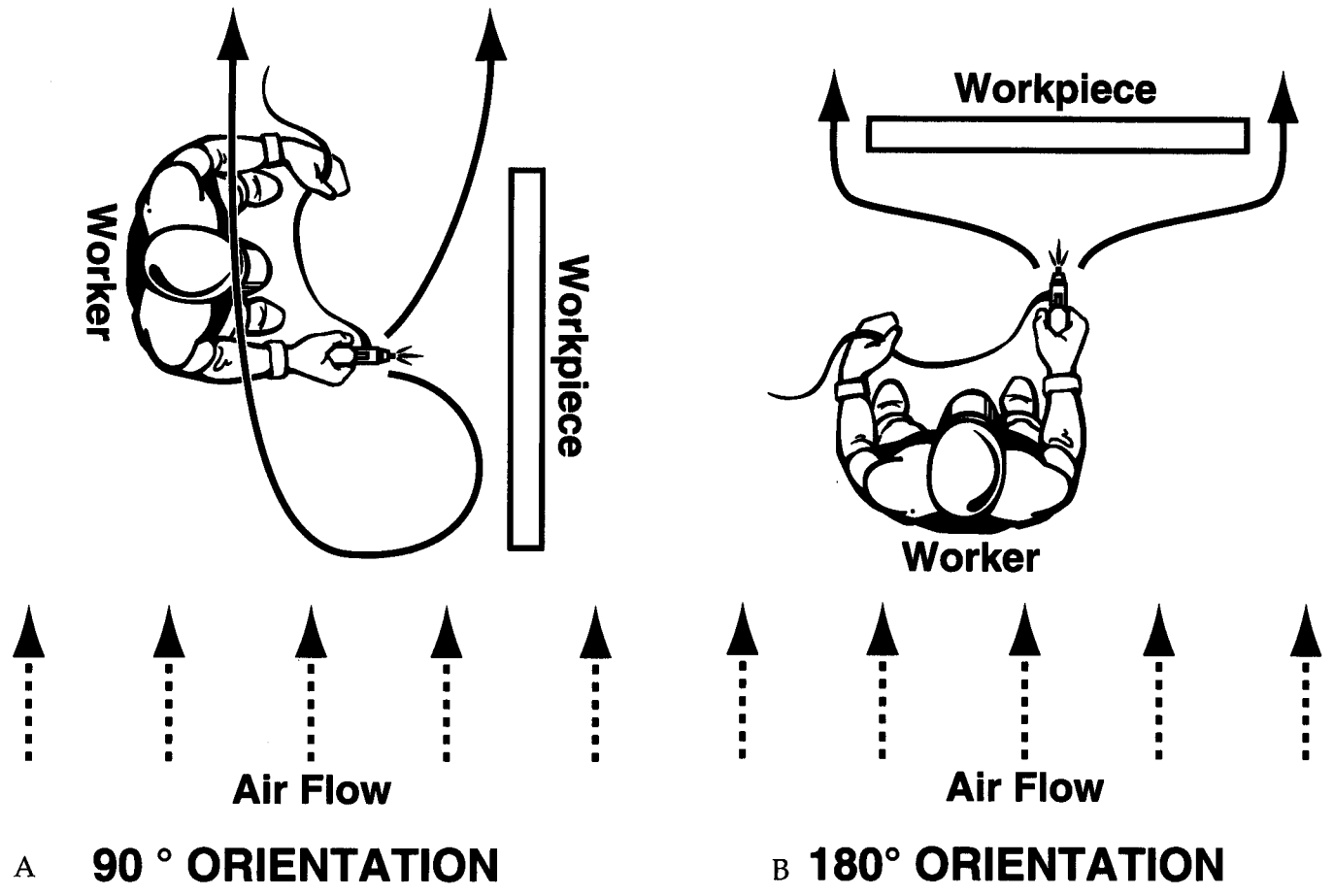

FIGURE 4. Path of the overspray for p_nH/μ_lU values greater than 5.0×10^6. In the 90° orientation the overspray passed directly through the mannequin's breathing zone, while in the 180° orientation the freestream captured the overspray before it could enter the breathing zone.

were less than an actual paint spray gun, scaling of the model may be a problem. Field studies are in progress to determine how well the model predicts worker exposures during actual spraying tasks and the importance of these limitations.

If validated in the field, the orientation effect may have important implications for conventional and HVLP spray painting. Conventional spraying typically operates at nozzle pressures and p_nH/μ_lU values to the right of the crossover point in Figure 3. This means worker breathing zone concentrations may be higher when spraying in the 90° orientation, and perhaps it is better to perform the task in the 180° orientation, at least from an exposure viewpoint. On the other hand, HVLP spray painting occurs at p_nH/μ_lU values to the left of the crossover point. This means the 90° orientation may result in lower breathing zone concentrations. Manufacturers claim HVLP spray guns reduce the mass generation rate of the overspray, but whether this leads to reduced worker exposures is questionable. The orientation effect could confound this assumption.

Conclusions

An empirical model based in dimensional analysis which predicts breathing zone concentrations of paint mist during spray painting tasks was developed in a laboratory wind tunnel using a mannequin, flat plate, and spray nozzle. The model indicates that the nondimensional breathing zone concentration $CUHD/m_o$ is a strong function of the quantity p_nH/μ_lU and worker orientation to the freestream. A significant interaction occurs between p_nH/μ_lU and worker orientation. All other factors being equal, breathing zone concentrations are higher in the 90° orientation when p_nH/μ_lU exceeds 5.0×10^6 but higher in the 180° orientation if p_nH/μ_lU is less than 5.0×10^6. The air-to-liquid mass flow ratio m_a/m_l does not significantly aid in predicting breathing zone concentrations in either orientation.

Field studies are in progress to determine whether the model can predict worker exposures during actual painting tasks. Differences between the laboratory setup and field painting tasks could limit the model. However, this research indicates the potential for an empirical–conceptual model to predict breathing zone concentrations and identify improved control methods.

Acknowledgments

NIOSH grant 5 R01 OH02858 partially supported this work. The authors also thank Neil McKenney for drawing the figures.

References

1. American Conference of Governmental Industrial Hygienists: Industrial Ventilation, A Manual of Recommended Practice. ACGIH, Cincinnati, OH (1995).
2. Kromhout, H.; Swuste, P.; Boleij, J.S.M.: Empirical Modelling of Chemical Exposure in the Rubber-Manufacturing Industry. Ann. Occup. Hyg. 38(1):3–22 (1994).
3. Woskie, S.R.; Smith, T.J.; Hammond, S.K.; Hallock, M.H.: Factors Affecting Worker Exposures to Metal-Working Fluids During Automotive Component Manufacturing. Appl. Occup. Environ. Hyg. 9(9):612–621 (1994).
4. Taylor, E.S.: Dimensional Analysis for Engineers. Clarendon Press, Oxford, UK (1974).
5. Hund, J.P.: Spray Application Processes. Metal Finishing: Organic Finishing Guidebook and Directory Issue 93(5A):97–111 (1993).
6. Bayvel, L.; Orzechowski, Z.: Liquid Atomization. Taylor and Francis, Washington, DC (1993).
7. Lefebvre, A.H.: Atomization and Sprays. Hemisphere Corp., New York (1989).
8. Kim, K.Y.; Marshall, W.R.: Drop-Size Distributions from Pneumatic Atomizers. AIChE J. 17(3):575–584 (1971).
9. Kwok, K.C.: A Fundamental Study of Air Spray Painting. Ph.D. thesis. University of Minnesota, Minneapolis, MN (1991).
10. Hicks, P.G.; Senser, D.W.: Simulation of Paint Transfer in an Air Spray Process. In: Fluid Mechanics and Heat Transfer in Sprays, FED-Vol. 178/HTD-Vol 270, pp. 145–154. American Society of Mechanical Engineers, New York (1993).
11. George, D.K.; Flynn, M.R.; Goodman, R.: The Impact of Boundary Layer Separation on Local Exhaust Design and Worker Exposure. Appl. Occup. Environ. Hyg. 5(8):501–509 (1990).
12. Kim, T.; Flynn, M.R.: Modeling a Worker's Exposure from a Hand-Held Source in a Uniform Freestream. Am. Ind. Hyg. Assoc. J. 52(11):456–463 (1991).
13. Flynn, M.R.; George, D.K.: Aerodynamics and Exposure Variability. Appl. Occup. Environ. Hyg. 6(1):36–39 (1991).
14. Flynn, M.R.; Shelton, W.K.: Factors Affecting the Design of Local Exhaust Ventilation for the Control of Contaminants from Hand-Held Sources. Appl. Occup. Environ. Hyg. 5(10):707–714 (1990).
15. O'Brien, D.M.; Hurley, D.E.: An Evaluation of Engineering Control Technology for Spray Painting. DHHS (NIOSH) Pub. No. 81–121. National Institute for Occupational Safety and Health, Cincinnati, OH (1981).
16. Cohen, B.S.; Brosseau, L.M.; Fang, C.P.; et al.: Measurement of Air Concentrations of Volatile Aerosols in Paint Spray Applications. Appl. Occup. Environ. Hyg. 7(8):514–521 (1992).
17. Whitehead, L.W.; Ball, G.L.; Fine, L.J.; Langolf, G.D.: Solvent Vapor Exposures in Booth Spray Painting and Spray Glueing, and Associated Operations. Am. Ind. Hyg. Assoc. J. 45(11):767–772 (1984).
18. Jayjock, M.A.; Levin, L.: Health Hazards in a Small Automotive Body Repair Shop. Ann. Occup. Hyg. 28(1):19–29 (1984).
19. Winder, C.; Turner, P.J.: Solvent Exposure and Related Work Practices Amongst Apprentice Spray Painters in Automotive Repair Workshops. Ann. Occup. Hyg. 36(4):385–394 (1992).
20. Garrett, J.W.; Kennedy, K.W.: A Collation of Anthropometry. Aerospace Medical Research Laboratory, Wright-Patterson AFB, OH (1971).
21. National Institute for Occupational Safety and Health: Particulates Not Otherwise Regulated, Total: Method 0500. In: NIOSH Manual of Analytical Methods, 4th ed. P.M. Eller, Ed. NIOSH, Cincinnati, OH (1994).
22. Willeke, K.; Baron, P.A.: Sampling and Interpretation Errors in Aerosol Monitoring. Am. Ind. Hyg. Assoc. J. 51(3):160–168 (1990).
23. Raynor, G.S.: Variation in Entrance Efficiency of a Filter Sampler with Air Speed, Flow Rate, Angle and Particle Size. Am. Ind. Hyg. Assoc. J. 31(3):294–304 (1970).
24. Mark, D.; Vincent, J.H.: A New Personal Sampler for Airborne Total Dust in Workplaces. Ann. Occup. Hyg. 30(1):89–102 (1986).
25. Buchan, R.M.; Soderholm, S.C.; Tillery, M.I.: Aerosol Sampling Efficiency of 37 mm Filter Cassettes. Am. Ind. Hyg. Assoc. J. 47(12):825–831 (1986).
26. Chung, K.Y.K.; Ogden, T.L.; Vaughan, N.P.: Wind Effects on Personal Dust Samplers. J. Aerosol Sci. 18(2):159–174 (1987).
27. Vincent, J.H.; Mark, D.: Entry Characteristics of Practical Workplace Aerosol Samplers in Relation to the ISO Recommendations. Ann. Occup. Hyg. 34(3):249–262 (1990).
28. Mark, D.: The Use of Dust-Collecting Cassettes in Dust Samplers. Ann. Occup. Hyg. 34(3):281–291 (1990).
29. Demange, M.; Gendre, J.C.; Herve-Bazin, B.; et al.: Aerosol Evaluation Difficulties Due to Particle Deposition on Filter Holder Inner Walls. Ann. Occup. Hyg. 34(4):399–403 (1990).
30. Lee, K.W.; Ramamurthi, M.: Filter Collection. In: Aerosol Measurement: Principles, Techniques, and Applications, pp. 179–205. K. Willeke and P. Baron, Eds. Van Nostrand Reinhold, New York (1993).
31. McAneny, J.J.; Leith, D.; Boundy, M.G.: Volatilization of Mineral Oil Mist Collected on Sampling Filters. Appl. Occup. Environ. Hyg. 10(9):783–787 (1995).
32. Beaulieu, H.J.; Fidino, M.S.; Arlington, K.L.B.; Buchan, R.M.: A Comparison of Aerosol Sampling Techniques: "Open" Versus "Closed-Face" Filter Cassettes. Am. Ind. Hyg. Assoc. J. 41(10): 758–765 (1980).
33. American Society of Mechanical Engineers: Measurement Uncertainty, Part 1: Instruments and Apparatus. ANSI/ASME PTC 19.1-1985. ASME, New York (1985).
34. Kim, T.; Flynn, M.R.: The Effect of Contaminant Source Momentum on a Worker's Breathing Zone Concentration in a Uniform Freestream. Am. Ind. Hyg. Assoc. J. 53(12):757–766 (1992).

Appendix: Uncertainty Analysis

Bias, Precision, and Uncertainty

The bias and precision errors of the nondimensional quantities, and their calculated uncertainties, were found according to the American National Standards Institute/American Society of Mechanical Engineers standard on measurement uncertainty. A summary of the analysis follows.

Measurement equipment is subject to two types of error: bias and precision. Bias (or fixed error) is the systematic error constant for the duration of the experiment. Calibration reduces bias, but never totally eliminates it. The bias limit (B), the upper limit of the bias error, is difficult to estimate, especially if special test data which provide bias information are unavailable. Estimates of B are usually based on instrument manufacturers' reports and other references.

Precision error (also called random error) is the closeness of agreement between repeated measurements of the same quantity. It is measured by the precision index (S_x), which is an estimate of the standard deviation in repeated measurements. Several ways to estimate S_x are outlined in the American National Standards Institute standard.

Table 2 lists the estimated relative bias and precision errors in the measured experimental quantities.

The 95 percent uncertainty in the measurement (assuming

TABLE 2. Estimated Bias and Precision Error in Measured Experimental Parameters (Percent)

Measured Parameter	Bias Error	Precision Error
C^A	<0.1	5.6
U^B	4.5	2.1
H^B	<0.1	0.2
D^B	0.4	0.8
$m_o{}^C$	<0.1	0.8
$p_n{}^C$	5.0	2.9
$\mu_1{}^C$	1.0	0.5
$m_a{}^B$	2.4	0.7
$m_l{}^C$	<0.1	0.6

[A]NIOSH sampling method.
[B]Estimate.
[C]Manufacturer's literature.

the error is symmetrical about the measurement mean) is defined as:

$$U(95\%) = [B^2 + (tS_x)^2]^{1/2} \quad \text{(A1)}$$

where t is the 97.5th percentile of the two-tailed t-distribution and is a function of the number of degrees of freedom used to calculate S_x. For large samples t approaches 1.96 and is usually approximated as 2.0 for simplicity.

Propagation of Error

Measurement errors are propagated through the functional relationship between a quantity and its parameters. Sensitivity is the error propagated due to errors in the parameters. For a quantity F, if

$$F = f(x_1, x_2, \ldots, x_j) \quad \text{(A2)}$$

then the relative sensitivity coefficient is

$$\Theta_i = \frac{\partial F/\partial x_i}{F/x_i} \quad \text{(A3)}$$

The bias and precision errors are propagated separately until combined into an uncertainty.

$$S_F = \left[\sum_{i=1}^{j} (\Theta_i S_{x_i})^2\right]^{1/2} \quad \text{(A4)}$$

$$B_F = \left[\sum_{i=1}^{j} (\Theta_i B_{x_i})^2\right]^{1/2} \quad \text{(A5)}$$

Sample Calculation

For the dimensionless quantity

$$\tilde{C} = \frac{CUHD}{m_o} \quad \text{(A6)}$$

$$B_{\tilde{C}} = \left[\left(\frac{\partial\tilde{C}/\partial C}{\tilde{C}/C} \times B_C\right)^2 + \left(\frac{\partial\tilde{C}/\partial U}{\tilde{C}/U} \times B_U\right)^2 + \left(\frac{\partial\tilde{C}/\partial H}{\tilde{C}/H} \times B_H\right)^2 + \left(\frac{\partial\tilde{C}/\partial D}{\tilde{C}/D} \times B_D\right)^2 + \left(\frac{\partial\tilde{C}/\partial m_o}{\tilde{C}/m_o} \times B_{m_o}\right)^2\right]^{1/2}$$

$$= [(1 \times 0.001)^2 + (1 \times 0.045)^2 + (1 \times 0.001)^2 + (1 \times 0.004)^2 + (1 \times 0.001)^2]^{1/2} = 0.045 = 4.5\% \quad \text{(A7)}$$

Similarly,

$$S_{\tilde{C}} = \left[\left(\frac{\partial\tilde{C}/\partial C}{\tilde{C}/C} \times S_C\right)^2 + \left(\frac{\partial\tilde{C}/\partial U}{\tilde{C}/U} \times S_U\right)^2 + \left(\frac{\partial\tilde{C}/\partial H}{\tilde{C}/H} \times S_H\right)^2 + \left(\frac{\partial\tilde{C}/\partial D}{\tilde{C}/D} \times S_D\right)^2 + \left(\frac{\partial\tilde{C}/\partial m_o}{\tilde{C}/m_o} \times S_{m_o}\right)^2\right]^{1/2}$$

$$= [(1 \times 0.056)^2 + (1 \times 0.021)^2 + (1 \times 0.002)^2 + (1 \times 0.008)^2 + (1 \times 0.008)^2]^{1/2} = 0.061 = 6.1\% \quad \text{(A8)}$$

The 95 percent uncertainty in the measured quantity $\tilde{C}$ is

$$U_{\tilde{C}}(95\%) = [(0.045)^2 + (2 \times 0.061)^2]^{1/2} = 0.130 = 13.0\%$$